View metadata, citation and similar papers at core.ac.uk
brought to you by CORE
provided by University of Brighton Research Portal

Joint 18th IHPC and 12th IHPS, Jeju, Korea, June 12-16, 2016

Experimental Tests on Sodium Thermosyphons

Tiago W. Uhlmann[1], Marcia B. H. Mantelli[1*], Miriam Manzoni[2], Marco Marengo[2], Per Eskilson[3]

[1] Heat Pipe Laboratory (Labtucal), Mechanical Engineering Department, Federal University of Santa Catarina, Florianópolis, Brazil
[2] Università degli Studi di Bergamo, Dept. of Eng. and App. Science, Italy; University of Brighton, School of Computing, Engineering and Mathematics, UK
[3] Cleanergy, Theres Svenssons gata 15, 417 55 Göteborg, Sweden

Abstract

Thermosyphon is a heat transfer device built from an evacuated tube filled with an appropriate volume of working fluid. It operates on a closed two-phase cycle and utilizes latent heat of vaporization and condensation to transfer heat. To understand and evaluate the behavior of sodium thermosyphons and their capacity to transfer heat under temperatures around 1000 °C, four thermosyphons were fabricated, charged, and tested on the Heat Pipe Laboratory, Brazil. Five tests were performed, using an induction heater as heat source. Four of those tests used a copper coil with flowing water as heat sink, while the other used just the environment, allowing heat to be transferred by natural convection and radiation. The temperature difference between inlet and outlet flowing water, the temperature of the external wall in several regions of the thermosyphons, and the mass flow rate of the cooling water were recorded. Two calculation methods to determine the heat transfer rate were applied to the collected data. For cooling by the copper coil heat sink, the forced convection heat absorbed by the flowing water through the coil, was calculated and assumed to be the heat transfer rate through the condenser wall. When the environment was used as the heat sink, the heat transfer rate of the thermosyphon to the ambient was calculated using a literature natural convection correlation and a radiation analytical model. The applications of such analytical methods allowed computing the maximum heat transfer rate of a thermosyphon with a difference of 2.3%, proving that both methods can be used to determine the heat transfer rate of the thermosyphon. Another important observation is that the thermosyphons with ratio between working fluid and evaporator volumes of 80% transferred more heat than ones with filling ratio of 100%.

Keywords: Filling ratio; High temperature; Sodium; Thermosyphon

1. INTRODUCTION

Thermosyphon is a heat transfer device built from an evacuated tube filled with an appropriate volume of working fluid. It operates on a closed two-phase cycle and utilizes the latent heat of vaporization and condensation to transfer heat, creating very small temperature gradients along the thermosyphon length [1, 2]. Different working fluids can be employed, depending on the working temperature level of the system. Water is an excellent fluid for operating on temperatures between 30 and 200 °C; whereas, for temperatures between 500 and 1200 °C, potassium and sodium are among the most suitable working fluids [3].

Most correlations developed to predict the thermosyphon coefficients of heat transfer in the evaporator and condenser were developed for water, refrigeration gases, or alcohols [4, 5] and might not be applicable to other fluids, especially those which start up is in solid state at room temperature, such as sodium. However, even when the appropriate heat transfer correlation is available [6], it is recommended to run experimental tests before using the correlation for designing equipments [7].

To understand and evaluate the behavior of sodium thermosyphons and their capacity to transfer heat under temperatures around 1000 °C, four thermosyphons were fabricated, charged, and tested on the Heat Pipe Laboratory (LABTUCAL) of the Federal University of Santa Catarina.

Charging procedures of sodium heat pipes and thermosyphons are available in the literature [3, 8, 9] and they have three characteristics in common; first, they require a controlled inert atmosphere to avoid sodium reaction with air and humidity; second, the construction of a specific filling rig is necessary; third, liquid sodium is introduced in the tube. In order to simplify the charging procedure, the fabrication process presented here does not require a specific filling rig and solid sodium is introduced in the tube [10].

2. THERMOSYPHON FABRICATION

The fabrication process can be divided in five steps as follows:

1. Material selection and tube cutting;
2. Tube cleaning;
3. One end smashing, welding and leakage test;
4. Solid sodium tube charging;
5. Vacuum, smashing and weld cutting.

*Corresponding author: marcia.mantelli@ufsc.br, Phone: +55 48 3721-9937

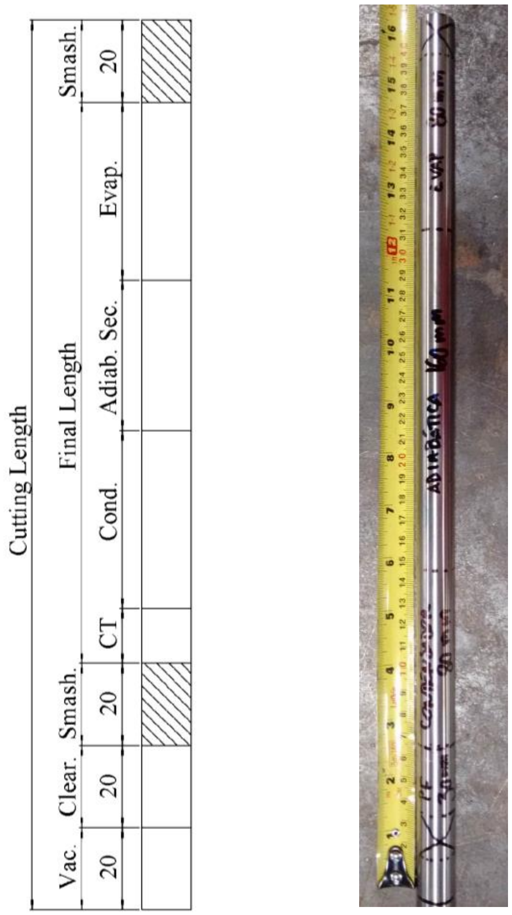

Fig. 1. Thermosyphon cutting length.

These steps will be explained in details in the following text. Table 1 lists the characteristics of the four thermosyphons fabricated through this process.

2.1 Material Selection and Tube Cutting

The tube material must be chosen according to the compatibility with the working fluid. Stainless steel and Inconel alloys are recommended for sodium [3]. In this work, Inconel 600 was used to fabricate the thermosyphons.

The thermosyphon tube cutting and final lengths are different due to the vacuum and smashing procedures. Evaporator, adiabatic section, condenser, and cold tip (CT) lengths compose the final length. Added to this, 40 mm are for smashing procedure, 20 mm for vacuum procedure, and 20 mm of clearance (Fig. 1).

2.2 Tube Cleaning

The tubes were washed with a solution of one part of an industrial degreasing (Quimatic ED Bio) to five parts of distilled water, thus rinsed with abundant distilled water. This process was repeated three times.

Fig. 2. Smashed tube end.

Fig. 3. Welded end.

2.3 One End Smashing, Welding, and Leakage Test

In order to close one side of the tube, the last 20 mm were smashed in a press with a load of 12 ton (Fig. 2). The smashed region was then TIG welded with a current of 70 A (Fig. 3) and a leakage test was performed in the tube using the equipment EDWARDS SPECTRON 5000 that detects traces of helium through its vacuum pumps and a helium detector. If no leakage was found, the tube was taken to the charging procedure.

2.4 Solid Sodium Tube Charging

The Sigma-Aldrich sodium used to charge the thermosyphons was 99.8% pure and was transported immerse in glass bottles with kerosene. In order to avoid the contamination of the glove box inert atmosphere with vapor of kerosene and air, the necessary amount of sodium was placed in a Kitasato flask and vacuum pumped (Fig. 4). Flask with sodium, Inconel tube (already subjected to the 2.1 to 2.3 steps), knife, silicon hoses, pressure scissors, scale, and tube diameter adapter were taken into a glove box filled with inert gas (Argon). Inside the glove box, the flask was opened and the external opaque sodium layer was removed (Fig. 5).

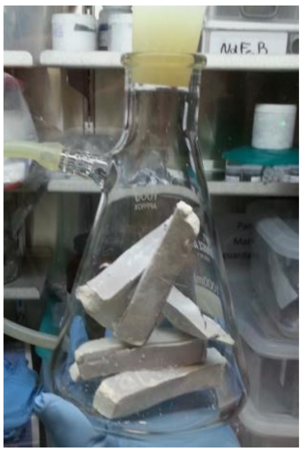

Fig. 4. Sodium in the Kitasato flask.

Fig. 5. Sodium with external layer partially removed.

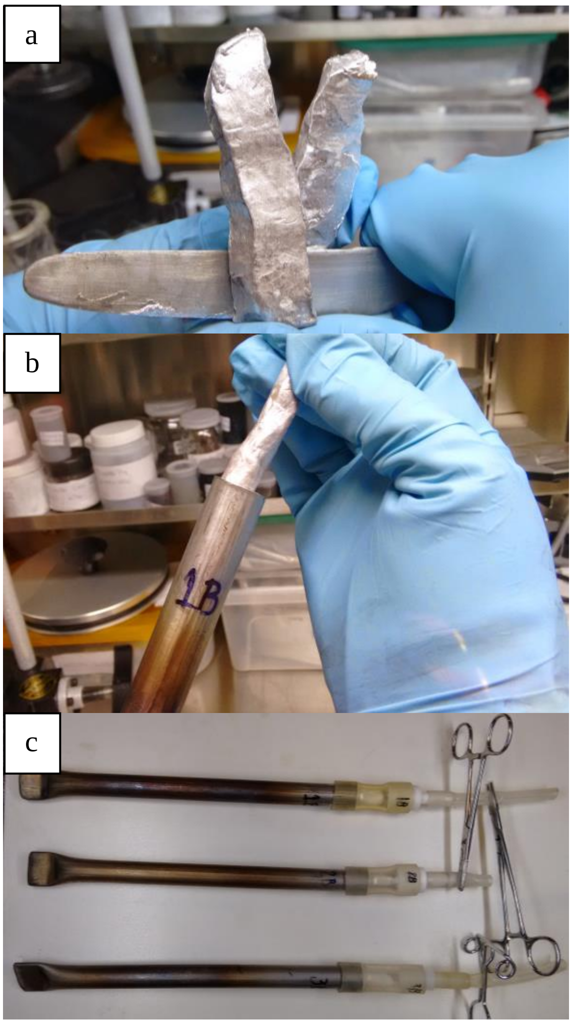

Fig. 6. Charging procedure. a) Cutting sodium in small pieces, b) inserting sodium in the tube, c) tube closed with silicon hoses, tube diameter adapter and pressure scissors.

Sodium was cut in small pieces, weighted, and introduced in the tube. The charged tube was closed with silicon hoses, tube diameter adapter and pressure scissors before has being removed from the glove box (Fig. 6.).

When the volume of sodium at room temperature was above around 22% of the total volume of the thermosyphon, it was necessary to heat up the tube above 98°C while charging with sodium to avoid sodium stacking.

2.5 Vacuum, Smashing and Weld Cutting

Outside the glove box, the tube was vacuum pumped up to 10^{-6} mbar to remove all gases. The silicon hose was closed again with the pressure scissor and the tube was smashed in a press in two steps; first, with a load of 16 ton with a plane mold; second, with a load of 10 ton with a wedge format mold (Fig. 7). In order to close the thermosyphon a

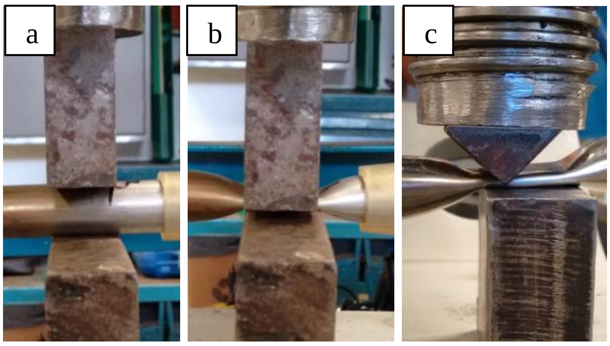

Fig. 7. Smashing. a) tube positioned between two plane molds, b) tube after 16 ton load, c) smashing with a load of 10 ton and a wedge form mold.

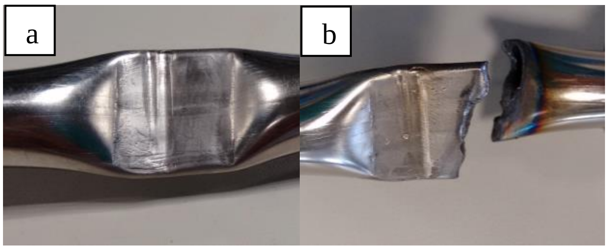

Fig. 8. Weld cutting. a) Before, b) after.

TIG weld cutting with a current of 100 A was performed (Fig. 8).

3. EXPERIMENTAL PROCEDURE AND DATA PROCESSING

Five tests were performed using the experimental procedure adopted in [10]. The induction coil used on tests (see Table 1) 1.1, 1.2, and 2 was of 100 mm of length and on tests 3 and 4 the induction coil was of 320 mm of length. All tests were in the vertical position.

In tests 1.2, 2, 3, and 4 the heat transfer rate was calculated through the copper coil calorimeter measurements using the known equation

$$Q = \dot{m} c_p \left(T_{out} - T_{in} \right). \qquad (1)$$

In test 1.1 the heat transfer rate was calculated considering natural convection and radiation to the environment. A correlation for natural convection in vertical cylinders presented by [11] was used to calculate the average coefficient of heat transfer considering the average condenser temperature as the cylinder wall temperature and the temperature of the environment as 30 °C. To calculate the total heat transfer rate through convection and radiation the condenser was divided in 6 parts, where each part was monitored by a thermocouple in the upper and lower regions. The average temperature between

Table 1. Thermosyphons and tests characteristics.

Test		1.1	1.2	2	3	4
Description		TS1	TS1	TS2	TS3	TS4
Tube Material		Inconel 600	Inconel 600	Inconel 600	Inconel 600	Inconel 600
Length [mm]	Evaporator	100	100	100	320	320
	Adiabatic Zone	0	85	85	0	0
	Condenser	145	35	35	124	124
	Cold Tip	0	25	25	25	25
	Total	245	245	245	469	469
Diameter [mm]	Inner	16	16	16	18	18
	Outer	18	18	18	21.34	21.34
Type of Condenser		Environment	Copper Coil	Copper Coil	Copper Coil	Copper Coil
Mass of Sodium (g)		20	20	15.6	78.8	62.1
Filling Ratio at Ambient Temperature		100%	100%	80%	100%	~80%
Maximum Calculated Heat Transfer Rate (W)		487	476	611	730	988
Induction coil current at Max. Calc. Heat Transfer Rate (A)		360	360	360	1660	1660

those two thermocouples was used to calculate the convection and radiation portion of each part. The thermosyphon was considered as a gray body with total hemispherical emissivity according to the linearization of the data presented in [12]:

$$\varepsilon_i = 0.0002 \cdot \overline{T}_i + 0.5734 \qquad (2)$$

and the total heat transfer rate of test 1.1 is given by:

$$Q = \sum_{i=1}^{6} hA_i \left(\overline{T}_i - T_\infty\right) + \sigma\varepsilon_i \left(\overline{T}_i^4 - T_\infty^4\right). \qquad (3)$$

The induction current used in tests 1.1, 1.2 and 2 did not reach the maximum possible induction coil current, but it was limited to 360 A, due to the high temperatures on the evaporator which would cause melting of the thermosyphon wall. In tests 3 and 4 the current of 1660 A was the maximum induction coil current used, which already caused overheating of the induction system. In average, each test last 50 minutes. In all tests, temperature gradients were observed along the thermosyphon, more evident in test 1.1, where heat was transferred to the ambient air.

4. TESTS RESULTS AND ANALYSIS

Fig. 9 shows the tested thermosyphon heat transfer rate as a function of its evaporator temperature for all tests performed. One can see that, for all tests, the thermosyphons only start to transfer more than 200 W after reaching 660 °C. Also, as the temperature of the evaporator increases, the heat transfer rates increases.

Tests with filling ratio (ratio between working fluid and evaporator volumes) of 80% (Test 2 and 4) transferred more heat than those with filling ratio of 100% (Tests 1.1, 1.2, 3), for a same evaporator temperature. It suggests that lower filling ratios are preferable. One reason for this best thermal behavior at lower filling ratio is that, in operation, the sodium expands, overpassing (flooding) the evaporator height. Note that the filling ratio was measured at room temperature. In tests 1.1 and 3, the height of the sodium pool reached the condenser, while in test 2 it reached the adiabatic section.

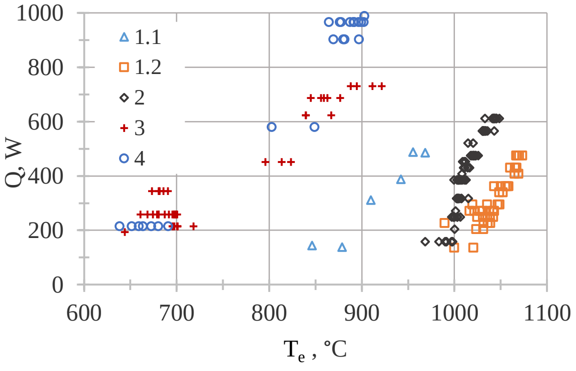

Fig. 9. Heat transfer rate versus temperature of the evaporator.

Table 2. Comparison between two calculation methods of heat transfer rate.

I (A)	Q (W) Test 1.1	Q (W) Test 1.2	Error
270	141	199	-29.0%
300	311	272	14.4%
330	387	351	10.4%
360	486	475	2.3%

In tests 1.1 and 1.2 (Thermosyphon 1), the same trend for the heat transfer rate increase is verified, but for different temperature levels. The lower temperature level on test 1.1 is attributed to the larger condenser area when compared with 1.2.

Table 2 brings a comparison between the two calculation methods for the heat transfer rate. The calorimeter results of test 1.2 are taken as the standard value for comparison. As the heat transfer rate increases, the error between methods decreases up to 2.3%, showing that both methods are consistent to calculate the maximum heat transfer rate. Also, for the tests when a calorimeter cannot be used, the heat transfer rate can be obtained applying the calculation method proposed for test 1.1, which shows a maximum error of 29.0%.

Test 1.1 presents a clear temperature gradient along the thermosyphon condenser (Fig. 10), with colder temperatures at the thermosyphon tip region. Two hypotheses can be proposed. First, the presence of non-condensable gases (NCG - air) that entered inside the thermosyphon during the last stage of the fabrication process. The NCG concentrates in the tube tip region, avoiding the thermosyphon working fluid to phase change, resulting, therefore, in a colder tip. Second, the heat removal rate is high enough to condense and decrease the sodium temperature on the condenser. As the temperature decreases, the pressure also decreases and the sodium cannot reach the thermosyphon condenser end. In both hypothesis only the heat transferred by conduction through the metallic tube wall is able to reach the condenser end. Further investigations of these hypotheses are recommended. The other tests presented a practically constant temperature before the condenser and a cold tip after.

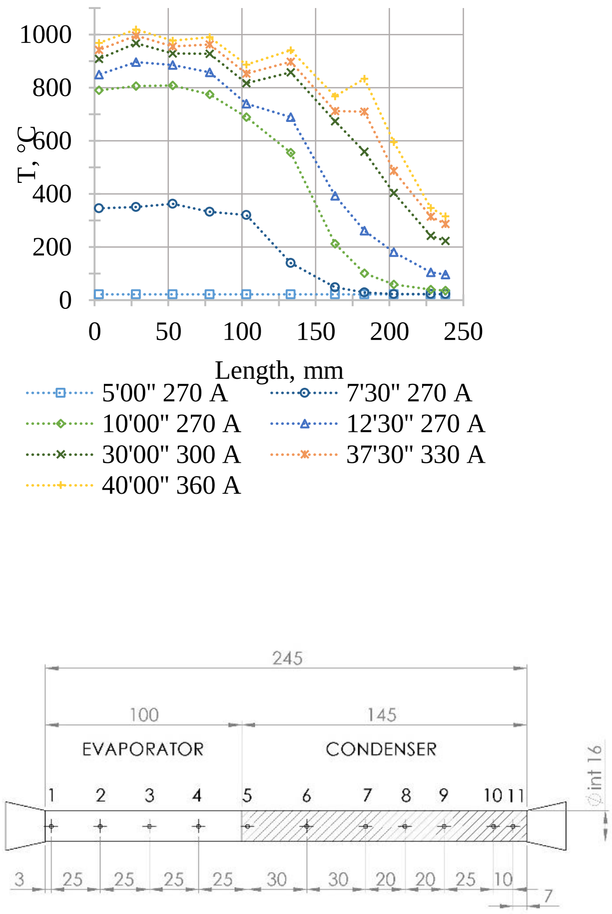

Fig. 10. External wall temperatures along the length for test 1.1.

5. CONCLUSIONS

Four sodium thermosyphons were fabricated, charged, and tested with success in the Heat Pipe Laboratory (Brazil). Five tests were performed with two different heat sinks. One test used the environment and the other four used a water calorimeter, made of a copper coil, as the heat sink. Two heat transfer rate calculation methods were compared and considered valid to calculate the maximum heat transfer rate, with an error of 2.3%.

To the same evaporator temperature, thermosyphons with filling ratio of 80% presented a higher heat transfer rate than ones with filling ratio of 100%, suggesting that lower filling ratios are preferable. A temperature gradient was observed and non-condensable gases or high heat removal were proposed as hypotheses that caused such gradient.

ACKNOWLEDGEMENT

The authors recognize the significant financial support given by Cleanergy AB (Sweden).

NOMENCLATURE

Q	:	Heat transfer rate (W)
$\dot{m}$	:	Mass flow rate of water (kg/s)
c_p	:	Specific heat of water (J/(kg.K))

T_{out} : Output temperature of water (K)

T_{in} : Input temperature of water (K)

ε_i : Total hemispherical emissivity of Inconel 600 (-)

$\bar{T}_i$: Average temperature of part *i* of the condenser (K)

h : Coefficient of heat transfer (W/(m^2.K))

A_i : External area of part *i* of the condenser (m^2)

T_∞ : Temperature of the environment (K)

T_e : Average temperature of the evaporator (°C)

REFERENCES

[1] Peterson, G.P., *An introduction to heat pipes: modeling, testing, and applications*, New York, Wiley-Interscience Publication, (1994).

[2] Mantelli, M.B.H., *Thermosyphon Technology for Industrial Applications, in Heat Pipes and Solid Sorption Transformations - Fundamentals and Practical Applications* by Vasiliev and Kakaç. 1st ed.: CRC Press, (2013), pp. 411.

[3] Reay, D. and Kew, P., *Heat Pipes: Theory, Design and Applications,* Burlington, Butterworth-Heinemann, 5th ed., (2006)

[4] Kaminaga, F., Okamoto, Y., Heat-transfer characteristics of two-phase thermosiphon heat pipe. Part 1. Boiling heat-transfer correlation in heating section, *Heat Transfer – Japanese Research*, vol. 23, pp. 52-65, (1994)

[5] Gross, U., Reflux condensation heat transfer inside a closed thermosyphon, *International Journal of Heat and Mass Transfer*, vol. 35, pp. 279-294, (1992)

[6] Shah, M. M. and A Survey of Experimental Heat Transfer Data for Nucleate Pool Boiling of Liquid Metals and a New Correlation, *International Journal of Heat and Fluid Flow*, vol. 13, pp. 370-379, (1992). http://dx.doi.org/10.1016/0142-727X(92)90007-V.

[7] Dobson, R. T. and Laubscher, R., Heat pipe heat exchanger for high temperature nuclear reactor technology, *Frontiers of Heat Pipes*, vol. 4, p. 1–7, (2013) http://dx.doi.org/10.5098/fhp.v4.2.3002.

[8] Faghri, A., *Heat pipe science and technology*, Taylor & Francis, USA, (1995).

[9] Dillig, M., Leimert, J. and Karl, J., Planar high temperature heat pipes for SOFC/SOEC stack applications, *Fundamentals & Developments of Fuel Cells Conference*, (2013).

[10] Manzoni, M., Uhlmann, T. W., Mantelli, M. B. H., Eskilson, P. and Marengo, M., Numerical Simulation of a Sodium Thermosyphon, *14th UK Heat Transfer Conference*, (2015).

[11] Nellis, G. and Klein, S., *Heat Transfer*, Cambridge University Press, (2006).,

[12] Inconel Alloy 600 Data Sheet. Available in http://www.specialmetals.com/assets/documents/alloys/inconel/inconel-alloy-600.pdf. Accessed in March, 11th 2016.